

# Low-PMEPR Rotatable Pilot Sequences for MIMO-OFDM Systems

Yajing Zhou · Zhi Gu · Zhengchun Zhou · Yang Yang

Received: date / Accepted: date

**Abstract** Multiple-input multiple-output orthogonal frequency division multiplexing (MIMO-OFDM) is the core of many advanced WiFi standards like IEEE 802.11n/ac to increase the throughput of WiFi. Operating at 5 GHz band and considering the phase tracking of the very high throughput long training field (VHT-LTF) sequences, MIMO-OFDM receivers are far more efficient in IEEE 802.11ac as compared to IEEE 802.11n. As per the functionalities of the IEEE 802.11ac standard, traditional preamble sequences may display intolerable peak-to-envelope power ratios (PMEPRs), if used as VHT-LTFs, due to phase rotation in pilot tones. In this paper, we focus on the construction of rotatable sequence sets (RSSs) of different sizes with low PMEPRs, where the proposed sequences can be efficiently used as VHT-LTFs in IEEE 802.11ac standard.

**Mathematics Subject Classification (2000)** 06E30 · 11T71 · 94A60

---

Yajing Zhou  
School of Information Science and Technology  
Southwest Jiaotong University  
Chengdu, China.  
E-mail: zhoyajing@my.swjtu.edu.cn

Zhi Gu  
School of Information Science and Technology  
Southwest Jiaotong University  
Chengdu, China.  
E-mail: goods@my.swjtu.edu.cn

Zhengchun Zhou  
School of Mathematics  
Southwest Jiaotong University  
Chengdu, China.  
E-mail: zzc@swjtu.edu.cn

Yang Yang  
School of Mathematics  
Southwest Jiaotong University  
Chengdu, China.  
E-mail: yayadata@swjtu.edu.cn

## 1 INTRODUCTION

Since its inception in 1997 [5], WiFi has been extensively used in modern communication systems. Rapid innovations in WiFi technology have contributed significantly to the Internet of Things (IoT). WiFi is based on the IEEE 802.11 standard family, which refers to a set of standards that define communication for wireless local area networks (WLANs) [5]. WiFi generally operates in two main frequencies: IEEE 802.11a [6] operates in 5 GHz and IEEE 802.11b [7] operates in 2.4 GHz. 2.4 GHz has been a common choice for WiFi users for long time since it works with most mainstream devices and is less expensive than 11a. In 2003, faster speeds and distance coverage of the earlier WiFi versions were combined to make the IEEE 802.11g standard [8]. IEEE 802.11n [1] was introduced in 2009, which was even faster and more reliable than its predecessor [1]. The efficiency of WiFi was drastically improved since IEEE 802.11n was enabled with multiple-input multiple-output orthogonal frequency division multiplexing (MIMO-OFDM) technology. This results to significant improvement in throughput without the using higher bandwidth or transmit power. However, due to low cost and popularity of the WiFi devices working in 2.4 GHz, large number of devices were using the same band, causing it to become overcrowded and slower. As a result, 5 GHz became the more attractive option. IEEE 802.11ac was introduced in 2012, which works on a 5 GHz band and is enabled with more efficient MIMO-OFDM receivers, making it much faster and more efficient compared to WiFi 802.11n. [11].

WiFi standards IEEE 802.11n/ac are OFDM enabled. The efficiency and cost of the OFDM receiver depends largely on the complexity of the implementation of the synchronization and channel estimation algorithms [13]. Higher efficiency is required in the synchronization process, since the coherent demodulation of OFDM is incredibly sensitive to such errors. Carrier and sampling frequency acquisition and maintenance with high precision are important for the successful transmission of long packets. Residual carrier frequency offset (CFO) and sampling frequency offset (SFO) tracking (phase tracking) are thus very critical part of OFDM receivers [13]. Initially MIMO-OFDM was used in IEEE 802.11n standard [1]. The MIMO technology used in IEEE 802.11n standard effectively implements multi-paths through space division multiplexing (SDMA) [1]. The data stream is being divided by the transmitter into multiple parts, known as spatial streams. Every spatial stream is transmitted through separate antennas to the corresponding receiver antennas. However, because of very high throughput (VHT) 5 GHz band and the growth of the number of spatial streams, the phase shift caused by residual CFO and phase noise are much more serious in very high throughput-long training fields (VHT-LTFs), which will lead to worse performance of MIMO channel estimation. Hence, it is necessary to do phase tracking during VHT-LTFs. Typically, pilot tones in data symbols have been used for phase tracking. However, in the case of 5 GHz band, phase tracking in this conventional way is very costly and not feasible during the MIMO channel estimation. Pilot tones as described in IEEE 802.11n for long training fields (LTF) differ from stream to stream and there-

fore can not be used for accurate phase tracking [1]. Another key problem for the implementation of OFDM is dealing with a relatively high level of peak-to-mean envelope power ratio (PMEPR) of the OFDM signal [14].

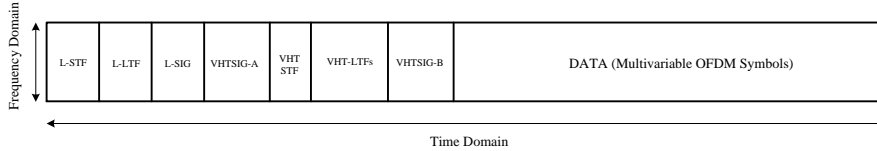


**Fig. 1** A physical layer coverage protocol frame format [15].

A typical physical layer coverage protocol frame format is shown in Figure 1. To enable phase tracking in IEEE 802.11ac, pilot tones are defined in VHT-LTF [2] similar to pilot tone in data symbols. Unlike the previous standard IEEE 802.11n, the MIMO training mapping cover sequence matrix (generally called the  $\mathbf{P}$  matrix) is not applied to the pilot tones during channel estimation based on pilot tones. Instead of that, single stream pilots are mapped to all space times streams (STs) [2]. To do this, the  $\mathbf{P}$  matrix is replaced by the  $\mathbf{R}$  matrix (receive signal matrix) where all rows of  $\mathbf{R}$  matrix are identical to the first row of the  $\mathbf{P}$  matrix [2]. A per stream cyclic shift delay (CSD) is applied to all streams after the  $\mathbf{R}$  mapping of the pilot tones of the VHT-LTF to avoid unwanted transmit beam forming. Pilot tones in the first VHT-LTF are used for initial one dimensional channel estimation. The pilot tones in the other remaining VHT-LTFs are used to estimate phase rotation based on pilot tones and the initial one dimensional channel estimation and correct the phase in data tones before MIMO channel estimation [2]. However, due to the dissimilarity between matrices  $\mathbf{P}$  and  $\mathbf{R}$  which results in the phase rotation in pilot tones of VHT-LTFs, the PMEPR of the VHT-LTFs may be intolerable. To the best of the authors' knowledge, lengths of VHT-LTFs in IEEE 802.11ac are 57, 117, 245, 501, which are very limited, and the indices of pilot tones are fixed for these lengths [2]. For example, in a 20 MHz transmission, the length of the VHT-LTF sequence is 57, where the pilot index set is  $\{7, 21, 35, 49\}$  [2].

This paper considers the design of VHT-LTF sequences in MIMO-OFDM systems, which can be used in the channel estimation in MIMO channels. Some general methods of generating RSSs whose pilot index sets are small are presented, which are available for 4-th rotatable index set. Then, we show that some CSSs can be used as the seed sequence sets to obtain new RSSs with larger lengths and pilot index set sizes.

## 1.1 Organization

The remaining paper is organized as follows. Section II gives the preliminaries used in the paper. In Section III, we present some general methods of generating RSS with small pilot sets and a method to construct RSSs with larger

lengths and larger sizes from some CSSs. We conclude the paper in Section IV.

We end this section by introducing some notations:

- $q$  is an even integer and  $\mathbb{Z}_q = \{0, 1, \dots, q-1\}$  denotes the ring of integers modulo  $q$ ;
- $\xi_q$  denotes the  $q$ -th primitive root of unity;
- $|a|$  and  $a^*$  denote the modulus and complex conjugation of complex number  $a$ , respectively;
- $\text{Re}(a)$  denotes the real part of the complex number  $a$ ;
- $|\mathbf{a}|$  denotes the magnitude of the vector  $\mathbf{a}$ .

## 2 PRELIMINARIES

### 2.1 Complementary Sequence Sets

Let  $\mathbf{a} = (a(0), a(1), \dots, a(L-1))$  and  $\mathbf{b} = (b(0), b(1), \dots, b(L-1))$  be complex-valued sequences of length  $L$ . The aperiodic cross-correlation between  $\mathbf{a}$  and  $\mathbf{b}$  at a time shift  $\tau$  is defined as

$$R_{\mathbf{a}, \mathbf{b}}(\tau) = \begin{cases} \sum_{i=0}^{L-1-\tau} a(i)b^*(i+\tau), & 0 \leq \tau \leq L-1; \\ \sum_{i=0}^{L-1+\tau} a(i-\tau)b^*(i), & -(L-1) \leq \tau \leq -1; \\ 0, & |\tau| \geq L. \end{cases} \quad (1)$$

When  $\mathbf{a} = \mathbf{b}$ , then it is called the aperiodic auto-correlation of  $\mathbf{a}$  and is denoted by  $R_{\mathbf{a}}(\tau)$ .

**Definition 1** ([16]) Let  $\mathcal{A} = (\mathbf{a}_i)_{i=1}^N$  be a set of  $N$  sequences of length  $L$ . It is said to be a complementary sequence set (CSS) of size  $N$  if  $\sum_{i=1}^N R_{\mathbf{a}_i}(\tau) = 0$  for  $0 < \tau < L$ . In this case, every  $\mathbf{a}_i$  in  $\mathcal{A}$  is called a complementary sequence (CS). In particular, when  $N = 2$ ,  $\mathcal{A}$  is called a Golay complementary pair (GCP), and each of the constituent sequences in this pair is called a Golay complementary sequence (GCS).

**Definition 2 (Golay Mates)** A GCP  $(\mathbf{c}, \mathbf{d})$  is called a Golay mate of GCP  $(\mathbf{a}, \mathbf{b})$  if

$$R_{\mathbf{a}, \mathbf{c}}(\tau) + R_{\mathbf{b}, \mathbf{d}}(\tau) = 0, \text{ for all } 0 \leq \tau < L. \quad (2)$$

**Definition 3** For a complex-valued sequence  $\mathbf{a} = (a(0), a(1), \dots, a(L-1))$  and a  $q$ -th rotatable index set  $\Gamma$ , define a sequence set  $\mathcal{A}_\Gamma$  as follows

$$\mathcal{A}_\Gamma = \begin{bmatrix} \mathbf{a}_{1-q}^\Gamma \\ \vdots \\ \mathbf{a}_0^\Gamma \\ \vdots \\ \mathbf{a}_{q-1}^\Gamma \end{bmatrix} = \begin{bmatrix} a_{1-q}^\Gamma(0), a_{1-q}^\Gamma(1), \dots, a_{1-q}^\Gamma(L-1) \\ \vdots \\ a_0^\Gamma(0), a_0^\Gamma(1), \dots, a_0^\Gamma(L-1) \\ \vdots \\ a_{q-1}^\Gamma(0), a_{q-1}^\Gamma(1), \dots, a_{q-1}^\Gamma(L-1) \end{bmatrix}_{(2q-1) \times L}, \quad (3)$$

where

$$\mathbf{a}_p^\Gamma(i) = \begin{cases} a(i), & i \notin \Gamma, \\ a(i) \cdot \xi_q^p, & i \in \Gamma. \end{cases} \quad (4)$$

Then,  $\mathcal{A}_\Gamma$  is called the rotatable sequence set (RSS) of  $\mathbf{a}$  corresponding to  $\Gamma$ . Note that  $\mathbf{a}_0^\Gamma = \mathbf{a}$  for any  $\Gamma$ , hence, we denote  $\mathbf{a}_0^\Gamma = \mathbf{a}$ . Every sequence  $\mathbf{a}_p^\Gamma$  ( $1 - q \leq p \leq q - 1$ ) in a RSS is called a rotatable sequence (RS). In particular, for a given  $P$ , if  $\text{PMEPR}(\mathbf{a}_p^\Gamma) \leq P$ , then  $\mathcal{A}_\Gamma$  is called a  $(q, \Gamma, L, P)$ -RSS. In line with the introduction,  $\Gamma$  can be thought of as the pilot index set and  $q = \dim \mathbf{P}$ .

**Proposition 1** For given two  $q$ -th rotatable index sets  $\Gamma$  and  $\Gamma'$ , let  $\Gamma' = \{0, 1, \dots, L-1\} \setminus \Gamma$ , we have  $\mathbf{a}_p^\Gamma = \mathbf{b}_{-p}^{\Gamma'}$ , where

$$\mathbf{b} = \mathbf{a} \cdot \xi_q^p = (a(0) \cdot \xi_q^p, a(1) \cdot \xi_q^p, \dots, a(L-1) \cdot \xi_q^p).$$

**Definition 4 (Insertion Function)** Consider a sequence  $\mathbf{a}$  of length  $N$ , given by  $(a(0), a(1), \dots, a(L-1))$ . Then  $\mathfrak{J}(\mathbf{a}, r, x)$ , given by

$$\mathfrak{J}(\mathbf{a}, r, x) = \begin{cases} (x, a(0), a(1), \dots, a(L-1)), & \text{if } r = 0, \\ (a(0), a(1), \dots, a(L-1), x), & \text{if } r = L, \\ (a(0), a(1), \dots, a(r-1), x, a(r), \dots, a(L-1)), & 0 < r < L, \end{cases} \quad (5)$$

is an insertion function which generates sequence of length  $(L+1)$  with element  $x$  at the  $r$ -th position [10, 4, 3].

## 2.2 PMEPRs of OFDM Symbols

Let us consider an  $L$ -sub-carrier OFDM system. For a complex-valued sequence  $\mathbf{a} = (a(0), a(1), \dots, a(L-1))$ , the transmitted OFDM signal is the real part of the complex envelope, which can be written as

$$S_{\mathbf{a}}(t) = \sum_{i=0}^{L-1} a(i) e^{2\pi(f_c + i\Delta f)t\sqrt{-1}}, \quad 0 \leq t < T, \quad (6)$$

where  $f_c$  denotes the carrier frequency and  $\Delta f = \frac{1}{T}$  denotes the subcarrier spacing, with  $T$  being the OFDM symbol duration. The sequence  $\mathbf{a}$  of length  $L$  is called the modulating codeword of the OFDM symbol.

The instantaneous power of an OFDM sequence (codeword)  $\mathbf{a}$  is given by

$$P_{\mathbf{a}}(t) = |S_{\mathbf{a}}(t)|^2 = R_{\mathbf{a}}(0) + 2\text{Re} \left( \sum_{\tau=1}^{L-1} R_{\mathbf{a}}(\tau) e^{2\pi(\tau\Delta f)t\sqrt{-1}} \right). \quad (7)$$

The PMEPR of the OFDM sequence  $\mathbf{a}$  is then defined as:

$$\text{PMEPR}(\mathbf{a}) = \frac{\sup_{t \in [0, T]} P_{\mathbf{a}}(t)}{P_{av}(\mathbf{a})}, \quad (8)$$

where  $P_{av}(\mathbf{a})$  is the average power of  $\mathbf{a}$ , and

$$P_{av}(\mathbf{a}) = \frac{1}{T} \int_{[0, T]} P_{\mathbf{a}}(t) dt = \|\mathbf{a}\|^2 = R_{\mathbf{a}}(0). \quad (9)$$

Accordingly, the PMEPR of a sequence set  $\mathcal{A} = \{\mathbf{a}_1, \mathbf{a}_2, \dots, \mathbf{a}_N\}$  is defined as

$$\text{PMEPR}(\mathcal{A}) = \max_{\mathbf{a}_i \in \mathcal{A}} \text{PMEPR}(\mathbf{a}_i). \quad (10)$$

Combining Eqs. (7) and (8), it can be derived that for sequence set  $\mathcal{A}$  of length  $L$ , we have

$$\text{PMEPR}(\mathbf{a}_i) \leq \frac{1}{R_{\mathbf{a}_i}(0)} \left( \sum_{k=1}^N R_{\mathbf{a}_k}(0) + 2 \sum_{\tau=1}^{L-1} \left| \sum_{k=1}^N R_{\mathbf{a}_k}(\tau) \right| \right) \quad (1 \leq i \leq N) \quad (11)$$

which implies the following lemma:

**Lemma 1** ([9]) *Let  $\mathcal{A}$  be a CSS of size  $N$  in which all the sequences have the same energy. Then the PMEPR of  $\mathcal{A}$  is upper bounded by  $N$ .*

Lemma 1 is useful to evaluate the PMEPR of a sequence in the sequel.

Note that  $\text{PMEPR}(\mathcal{A}_\Gamma)$  may become much larger when the rotation set  $\Gamma$  is unsuitable for  $\mathbf{a}$ , which can be observed from the following example.

*Example 1* Let  $\mathbf{a} = (1, 1, 1, -1, 1, 1, -1, 1, 1, 1, 1, -1, -1, -1, 1, -1)$  and  $q = 4$ . Let  $\Gamma = \{4, 7, 12, 13, 14, 16\}$  be  $q$ -th rotatable index set, then,

$$\mathbf{a}_p^\Gamma = (1, 1, 1, -\xi_4^p, 1, 1, -\xi_4^p, 1, 1, 1, 1, -\xi_4^p, -\xi_4^p, -\xi_4^p, 1, -\xi_4^p), \quad (12)$$

here the elements marked in red are different from those in  $\mathbf{a}$  and  $1 \leq p \leq 3$ . Table 1 shows the PMEPRs of  $\mathbf{a}_p^\Gamma$  where  $0 \leq p \leq 3$ . It can be observed that  $\text{PMEPR}(\mathcal{A}_\Gamma) = 16.0000$ , which is equal to the length of  $\mathbf{a}$ .

**Table 1** PMEPR( $\mathbf{a}_p^\Gamma$ ) in Example 1 for  $p = 1, 2, 3$  and  $\Gamma$

$p$	$p = 0$	$p = 1$	$p = 2$	$p = 3$
$\text{PMEPR}(\mathbf{a}_p^\Gamma)$	1.7071	8.5000	16.0000	8.5000

Example 1 motivates us to search some RSS with low PMEPRs.

### 3 Proposed Low-PMEPR Training Sequences for Rotatable Pilots

In this section, first, we introduce some general methods of generating RSSs for 4-th rotatable index sets with small sizes from CSSs. Then, a general method about RSSs from some CSSs is also given.

#### 3.1 General Methods of Constructing RSSs for Small 4-th Rotatable Index Sets with Low PMEPRs

**Theorem 1** Consider  $q = 4$  and  $(\mathbf{a}, \mathbf{b})$  be a GCP of length  $L$  with  $(\mathbf{c}, \mathbf{d})$  be its Golay mate and these sequences have the same energy. Let  $\mathbf{e} = \mathfrak{J}(\mathbf{a}, 0, \xi_q)$  and  $\mathbf{h} = \mathfrak{J}(\mathbf{a}, L, \xi_q)$ . Also, let  $\mathbf{w} = (\mathbf{a} \parallel \mathbf{c})$  be sequence of length  $2L$  and  $\mathbf{k} = \mathfrak{J}(\mathbf{w}, L, \xi_q)$ . Then, we have the following results:

1. For 4-th rotatable set  $\Gamma = \{0\}$ ,  $\mathcal{E}_\Gamma$  is a  $(4, \Gamma, L + 1, 4)$ -RSS.
2. For 4-th rotatable set  $\Gamma = \{L\}$ ,  $\mathcal{H}_\Gamma$  is a  $(4, \Gamma, L + 1, 4)$ -RSS.
3. For 4-th rotatable set  $\Gamma = \{L\}$ ,  $\mathcal{K}_\Gamma$  is a  $(4, \Gamma, 2L + 1, 4)$ -RSS.
4. For 4-th rotatable set  $\Gamma = \{0, L + 1\}$  and  $\mathbf{m} = \mathfrak{J}(\mathbf{e}, L + 1, \xi_4)$ ,  $\mathcal{M}_\Gamma$  is a  $(4, \Gamma, L + 2, 4)$ -RSS.

To prove Theorem 1, we need the following results.

**Theorem 2 (Theorem 1 of [3])** Consider a GCP  $(\mathbf{a}, \mathbf{b})$  of length  $L$ . Let  $(\mathbf{c}, \mathbf{d})$  be its Golay mate. If  $x_1, y_1, x_2, y_2 \in \mathbb{U} = \{1, \xi_4^1, \xi_4^2, \xi_4^3\}$  and  $\mathbf{e} = \mathfrak{J}(\mathbf{a}, 0, x_1)$ ,  $\mathbf{f} = \mathfrak{J}(\mathbf{b}, 0, y_1)$ ,  $\mathbf{g} = \mathfrak{J}(\mathbf{c}, L, x_2)$ ,  $\mathbf{h} = \mathfrak{J}(\mathbf{d}, L, y_2)$ . Then  $\mathbf{A} = [\mathbf{e}, \mathbf{f}, \mathbf{g}, \mathbf{h}]^T$  is a CS of set size 4 and sequence length  $L + 1$  when  $x_1 = y_2$  and  $y_1 = -x_2$ .

**Theorem 3 (Theorem 2 of [3])** Consider a GCP  $(\mathbf{a}, \mathbf{b})$  of length  $L$ . Let  $(\mathbf{c}, \mathbf{d})$  be its Golay mate. Also let  $\mathbf{e} = \mathbf{a} \parallel \mathbf{c}$  and  $\mathbf{f} = \mathbf{b} \parallel \mathbf{d}$  be sequences of length  $2L$ . If  $x_1, y_1, x_2, y_2 \in \mathbb{U} = \{1, \xi_4^1, \xi_4^2, \xi_4^3\}$  and  $\mathbf{p} = \mathfrak{J}(\mathbf{e}, L, x_1)$ ,  $\mathbf{q} = \mathfrak{J}(\mathbf{f}, L, y_1)$ ,  $\mathbf{r} = \mathfrak{J}(\mathbf{e}, L, x_2)$ ,  $\mathbf{s} = \mathfrak{J}(\mathbf{f}, L, y_2)$ . Then  $\mathbf{A} = [\mathbf{p}, \mathbf{q}, \mathbf{r}, \mathbf{s}]^T$  is a CS of set size 4 and sequence length  $2L + 1$  when the following conditions hold.

$$x_1^* - y_1 + x_2^* - y_2 = 0, \quad x_1 + y_1^* + x_2 + y_2^* = 0. \quad (13)$$

**Theorem 4 (Theorem 3 of [3])** Consider a GCP  $(\mathbf{a}, \mathbf{b})$  of length  $L$ . Let  $(\mathbf{c}, \mathbf{d})$  be its Golay mate. Also, let  $x_1, y_1, x_2, y_2, x_3, y_3, x_4, y_4 \in \mathbb{U} = \{1, \xi_4^1, \xi_4^2, \xi_4^3\}$  and  $\mathbf{e} = \mathfrak{J}(\mathbf{a}, 0, x_1)$ ,  $\mathbf{f} = \mathfrak{J}(\mathbf{b}, 0, y_1)$ ,  $\mathbf{g} = \mathfrak{J}(\mathbf{c}, 0, x_3)$ ,  $\mathbf{h} = \mathfrak{J}(\mathbf{d}, 0, y_3)$ . If  $\mathbf{p} = \mathfrak{J}(\mathbf{e}, L + 1, x_2)$ ,  $\mathbf{q} = \mathfrak{J}(\mathbf{f}, L + 1, y_2)$ ,  $\mathbf{r} = \mathfrak{J}(\mathbf{g}, L + 1, x_4)$ ,  $\mathbf{s} = \mathfrak{J}(\mathbf{h}, L + 1, y_4)$ . Then  $\mathbf{A} = [\mathbf{p}, \mathbf{q}, \mathbf{r}, \mathbf{s}]^T$  is a CS of set size 4 and sequence length  $L + 2$  when the following set of conditions hold

$$x_1 - y_4^* = 0; \quad x_2^* - y_3 = 0; \quad y_1 + x_4^* = 0; \quad y_2^* + x_3 = 0. \quad (14)$$

Now, we are ready to prove Theorem 1.

*Proof of Theorem 1:*

1. For any  $c \in \mathbb{Z}_4$ , let  $\mathbf{e} = \mathcal{J}(\mathbf{a}, 0, \xi_q^c)$ ,  $\mathbf{e}_1 = \mathcal{J}(\mathbf{b}, 0, \xi_q^c)$ ,  $\mathbf{e}_2 = \mathcal{J}(\mathbf{c}, L, -\xi_q^c)$  and  $\mathbf{e}_3 = \mathcal{J}(\mathbf{d}, L, \xi_q^c)$ , then, according to Theorem 2, it can be obtained that  $\{\mathbf{e}, \mathbf{e}_1, \mathbf{e}_2, \mathbf{e}_3\}$  is a CS of length  $L + 1$ .
2. For any  $c \in \mathbb{Z}_4$ , let  $\mathbf{h} = \mathcal{J}(\mathbf{a}, L, \xi_q^c)$ ,  $\mathbf{h}_1 = \mathcal{J}(\mathbf{b}, L, \xi_q^c)$ ,  $\mathbf{h}_2 = \mathcal{J}(\mathbf{c}, 0, -\xi_q^c)$  and  $\mathbf{h}_3 = \mathcal{J}(\mathbf{d}, 0, \xi_q^c)$ , then, according to Theorem 2, we have  $\{\mathbf{h}, \mathbf{h}_1, \mathbf{h}_2, \mathbf{h}_3\}$  is a CS of length  $L + 1$ .
3. For any  $c \in \mathbb{Z}_4$ , let  $\mathbf{k} = \mathcal{J}(\mathbf{w}, L, \xi_q^c)$ ,  $\bar{\mathbf{w}} = (\mathbf{b} \parallel \mathbf{d})$  and  $\mathbf{k}_1 = \mathcal{J}(\bar{\mathbf{w}}, L, \xi_q^{-c})$ . Furthermore, let  $\mathbf{k}_2 = \mathcal{J}(\mathbf{w}, L, -\xi_q^c)$  and  $\mathbf{k}_3 = \mathcal{J}(\bar{\mathbf{w}}, L, -\xi_q^{-c})$ , then, according to Theorem 3, we have  $\{\mathbf{k}, \mathbf{k}_1, \mathbf{k}_2, \mathbf{k}_3\}$  is a CS of length  $2L + 1$ .
4. For any  $c \in \mathbb{Z}_4$ , let  $\mathbf{e} = \mathcal{J}(\mathbf{a}, 0, \xi_q^c)$ ,  $\mathbf{e}_1 = \mathcal{J}(\mathbf{b}, 0, -\xi_q^{-c})$ ,  $\mathbf{e}_2 = \mathcal{J}(\mathbf{c}, 0, \xi_q^c)$  and  $\mathbf{e}_3 = \mathcal{J}(\mathbf{d}, 0, \xi_q^{-c})$ . Also, let  $\mathbf{m} = \mathcal{J}(\mathbf{e}, L + 1, \xi_q^c)$ ,  $\mathbf{m}_1 = \mathcal{J}(\mathbf{e}_1, L + 1, -\xi_q^{-c})$ ,  $\mathbf{m}_2 = \mathcal{J}(\mathbf{e}_2, L + 1, \xi_q^c)$  and  $\mathbf{m}_3 = \mathcal{J}(\mathbf{e}_3, L + 1, \xi_q^{-c})$ , it can be verified from Theorem 4 that  $\{\mathbf{m}, \mathbf{m}_1, \mathbf{m}_2, \mathbf{m}_3\}$  is a CS of length  $L + 2$ .

The results can be derived from the argument above along with the condition that  $\mathbf{a}, \mathbf{b}, \mathbf{c}$  and  $\mathbf{d}$  have the same energy.

This proof is completed.

The pilot index sets Theorem 1 are very small, which may be not enough for phase tracking. The following result gives a new general method of generating CSSs from given ones, which can be used to obtain new RSSs with larger sequence lengths and pilot index sets.

### 3.2 General Methods of Constructing $q$ -th RSSs from CSSs

The following result about CSSs is straightforward from the Rudin-Shapiro polynomials in [12].

**Lemma 2** For  $M, N$  are positive integer with  $M = 2N$ , let  $\mathcal{S}^0 = \{\mathbf{s}_1^0, \mathbf{s}_2^0, \dots, \mathbf{s}_M^0\}$  be a CSS of length  $L$ . Then, a CSS  $\mathcal{S}^k = \{\mathbf{s}_1^k, \mathbf{s}_2^k, \dots, \mathbf{s}_M^k\}$  of length  $2^k L$  with size  $M$  can be constructed using the following two recursive formulas:

1.  $\mathbf{s}_{2n-1}^k = \mathbf{s}_{2n-1}^{k-1} \diamond \mathbf{s}_{2n}^{k-1}$ ,  $\mathbf{s}_{2n}^k = \mathbf{s}_{2n-1}^{k-1} \diamond -\mathbf{s}_{2n}^{k-1}$ ;
2.  $\mathbf{s}_{2n-1}^k = (\mathbf{s}_{2n-1}^{k-1} \parallel \mathbf{s}_{2n}^{k-1})$ ,  $\mathbf{s}_{2n}^k = (\mathbf{s}_{2n-1}^{k-1} \parallel -\mathbf{s}_{2n}^{k-1})$ ,

where  $n \in \{1, 2, \dots, N\}$ , “ $\diamond$ ” denotes the bit-interleaved operation and “ $\parallel$ ” denotes the concatenation operation.

**Theorem 5** With the same notation as Lemma 2, and for positive integers  $L, q$ , let  $\mathcal{S} = \{\mathbf{s}_1, \mathbf{s}_2, \dots, \mathbf{s}_M\}$  be a CSS of length  $L$  where the sequences have the same energy with  $M$   $q$ -th rotatable index sets

$$\Gamma_m = \{\{t_1^m, t_2^m, \dots, t_{d_m}^m\} : 1 \leq t_i^m \leq L\}, \quad (1 \leq m \leq M),$$

where  $|\Gamma_m| = d_m \geq 0$ . If for any  $p \in \mathbb{Z}_q$ ,  $S_p = \{\mathbf{s}_{1,p}^{\Gamma_1}, \mathbf{s}_{2,p}^{\Gamma_2}, \dots, \mathbf{s}_{M,p}^{\Gamma_M}\}$  is also a CSS, then, we have the following results.

1. If  $\mathcal{S}^k = \{\mathbf{s}_1^k, \mathbf{s}_2^k, \dots, \mathbf{s}_M^k\}$  be the sequence set generated in 1) in Lemma 2, and denote  $\mathbf{a} = \mathbf{s}_1^k$ , then,  $\mathcal{A}_{\Gamma^k}$  is a  $(q, \Gamma_1^k, 2^k L, M)$ -RSS where  $\Gamma_1^k = \Gamma_2^k = (2\Gamma_1^{k-1} - 1) \cup (2\Gamma_2^{k-1})$  with  $|\Gamma_1^k| = |\Gamma_2^k| = |\Gamma_1^{k-1}| + |\Gamma_2^{k-1}|$  ( $k \geq 1$ ) and  $\Gamma_1^0 = \Gamma_1, \Gamma_2^0 = \Gamma_2$ .

2. If  $\mathcal{S}^k = \{\mathbf{s}_1^k, \mathbf{s}_2^k, \dots, \mathbf{s}_M^k\}$  be the sequence set generated in 2) in Lemma 2, and denote  $\mathbf{a} = \mathbf{s}_1^k$ , then,  $\mathcal{A}_{\Gamma_1^k}$  is a  $(q, \Gamma_1^k, 2^k L, M)$ -RSS where  $\Gamma_1^k = \Gamma_2^k = \Gamma_1^{k-1} \cup (2^{k-1}L + \Gamma_2^{k-1})$  with  $|\Gamma_1^k| = |\Gamma_2^k| = |\Gamma_1^{k-1}| + |\Gamma_2^{k-1}|$  ( $k \geq 1$ ) and  $\Gamma_1^0 = \Gamma_1, \Gamma_2^0 = \Gamma_2$ .

*Proof* The proof of Theorem 5 is straightforward according to Lemma 2, so we omit it here.

*Remark 1* If the given CSS satisfies the condition in Theorem 5, new RSSs can be generated by all the general methods of CSSs based on existing CSSs using the given CSSs. The CSSs in Theorem 2 can be used as the seed CSS of Theorem 5, which can enlarge the sequence length along with larger rotatable index set size.

*Example 2* Taking  $\{(1, 1), (1, -1)\}$  as the GCP with  $\{(-1, 1), (-1, -1)\}$  be its Golay mate. Let

$$\mathbf{e} = (1, 1, 1), \mathbf{f} = (-1, 1, -1), \mathbf{g} = (1, 1, -1), \mathbf{h} = (-1, -1, -1),$$

and  $\Gamma_1 = \Gamma_2 = \{0\}, \Gamma_3 = \Gamma_4 = \{2\}$ , then, it can be easily checked that for any  $p \in \mathbb{Z}_4$ ,  $\{\mathbf{e}_p^{\Gamma_1}, \mathbf{f}_p^{\Gamma_2}, \mathbf{g}_p^{\Gamma_3}, \mathbf{h}_p^{\Gamma_4}\}$  is a CSS where

$$\mathbf{e}_p^{\Gamma_1} = (\xi_4^p, 1, 1), \mathbf{f}_p^{\Gamma_2} = (-\xi_4^p, 1, -1), \mathbf{g}_p^{\Gamma_3} = (1, 1, -\xi_4^p), \mathbf{h}_p^{\Gamma_4} = (-1, -1, -\xi_4^p).$$

Consider  $\mathbf{a} = \mathbf{e} \diamond \mathbf{f} = (1, -1, 1, 1, -1)$  and  $\tilde{\mathbf{a}} = \mathbf{e} \parallel \mathbf{f} = (1, 1, 1, -1, -1)$ , Tables 2 and 3 show the PMEPR of  $\mathbf{a}_p^{\Gamma}$  and  $\tilde{\mathbf{a}}_p^{\Gamma}$ , it can be observed that  $\{\mathbf{a}^{\Gamma}, \mathbf{a}_1^{\Gamma}, \mathbf{a}_2^{\Gamma}, \mathbf{a}_3^{\Gamma}\}$  is a  $(4, \{0, 1\}, 6, 2.6667)$ -RSS and  $\{\tilde{\mathbf{a}}^{\Gamma}, \tilde{\mathbf{a}}_1^{\Gamma}, \tilde{\mathbf{a}}_2^{\Gamma}, \tilde{\mathbf{a}}_3^{\Gamma}\}$  is a  $(4, \{0, 3\}, 6, 2.6667)$ -RSS.

**Table 2** PMEPR( $\mathbf{a}_p^{\Gamma}$ ) in Example 2 for  $p = 1, 2, 3$

$\frac{\text{PMEPR}(\mathbf{a}_p^{\Gamma})}{\Gamma}$	$p$			
	$p = 0$	$p = 1$	$p = 2$	$p = 3$
$\Gamma = \{0, 1\}$	2.6667	1.9107	2.0000	1.9107

**Table 3** PMEPR( $\tilde{\mathbf{a}}_p^{\Gamma}$ ) in Example 2 for  $p = 1, 2, 3$

$\frac{\text{PMEPR}(\tilde{\mathbf{a}}_p^{\Gamma})}{\Gamma}$	$p$			
	$p = 0$	$p = 1$	$p = 2$	$p = 3$
$\Gamma = \{0, 3\}$	2.6667	2.4880	2.0000	2.4880

## 4 Concluding Remarks

In this paper, we have designed sequences which can efficiently handle the phase rotation necessary for MIMO-OFDM channel estimation in IEEE 802.11ac standards, having low PMEPR bounds. We have proposed some methods of generating RSSs with low PMEPRs for small 4-th rotatable index sets, followed by a method of RSSs with larger lengths and pilot sets from certain CSSs. These sequences can be efficiently used as VHT-LTF sequences in IEEE 802.11ac standards, which uses MIMO-OFDM technique for efficient communication.

## References

1. IEEE standard for information technology—local and metropolitan area networks—specific requirements—part 11: Wireless lan medium access control (mac) and physical layer (phy) specifications amendment 5: Enhancements for higher throughput. IEEE Std 802.11n<sup>TM</sup>-2009 (Amendment to IEEE Std 802.11-2007 as amended by IEEE Std 802.11k-2008, IEEE Std 802.11r-2008, IEEE Std 802.11y-2008, and IEEE Std 802.11w-2009) pp. 1–565 (2009). DOI 10.1109/IEEESTD.2009.5307322
2. IEEE Standard for Information technology—Telecommunications and information exchange between systems—Local and metropolitan area networks—Specific requirements—Part 11: Wireless LAN Medium Access Control (MAC) and Physical Layer (PHY) Specifications—Amendment 4: Enhancements for Very High Throughput for Operation in Bands below 6 GHz. IEEE Std 802.11ac<sup>TM</sup>-2013 (Amendment to IEEE Std 802.11-2012, as amended by IEEE Std 802.11ae-2012, IEEE Std 802.11aa-2012, and IEEE Std 802.11ad-2012) pp. 1–425 (2013)
3. Adhikary, A.R., Majhi, S.: New constructions of complementary sets of sequences of lengths non-power-of-two. *IEEE Commun. Lett.* **23**(7), 1119–1122 (2019)
4. Adhikary, A.R., Majhi, S., Liu, Z., Guan, Y.L.: New sets of even-length binary Z-complementary pairs with asymptotic ZCZ ratio of 3/4. *IEEE Signal Process. Lett.* **25**(7), 970–973 (2018)
5. Hanzo, L., Akhtman, Y.J., Wang, L., Jiang, M.: MIMO OFDM for LTE, WiFi and WiMAX: Coherent versus Noncoherent and Cooperative Turbo Transceivers. John Wiley and Sons, Ltd (2010)
6. Institute of Electrical and Electronics Engineers: Supplement to IEEE Standard for Information Technology—Telecommunications and Information Exchange Between Systems—Local and Metropolitan Area Networks—Specific Requirements—Part 11: Wireless LAN Medium Access Control (MAC) and Physical Layer (PHY) Specifications: High-speed Physical Layer in the 5 GHz Band. IEEE 802.11a-1999 (1999)
7. Institute of Electrical and Electronics Engineers: Supplement to IEEE Standard for Information Technology—Telecommunications and Information Exchange Between Systems—Local and Metropolitan Area Networks—Specific Requirements—Part 11: Wireless LAN Medium Access Control (MAC) and Physical Layer (PHY) Specifications: Higher-speed Physical Layer Extension in the 2.4 GHz Band. IEEE 802.11b-1999 (1999)
8. Institute of Electrical and Electronics Engineers: IEEE Standard for Information Technology—Telecommunications and Information Exchange Between Systems—Local and Metropolitan Area Networks—Specific Requirements—Part 11: Wireless LAN Medium Access Control (MAC) and Physical Layer (PHY) Specifications—Amendment 4: Further Higher Data Rate Extension in the 2.4 GHz Band. IEEE 802.11g-2003 (2003)
9. Liu, Z., Guan, Y.L.: 16-QAM almost-complementary sequences with low PMEPR. *IEEE Trans. Commun.* **64**(2), 668–679 (2016)
10. Liu, Z., Paramalli, U., Guan, Y.L.: Optimal odd-length binary Z-complementary pairs. *IEEE Trans. Inf. Theory* **60**(9), 5768–5781 (2014)

- 
11. Rochim, A.F., Sari, R.F.: Performance comparison of ieee 802.11n and ieee 802.11ac. In: 2016 International Conference on Computer, Control, Informatics and its Applications (IC3INA), pp. 54–59 (2016)
  12. Rudin, W.: Some theorems on Fourier coefficients. *Proc. Amer. Math. Soc.* **10**, 855–859 (1959)
  13. S. S. Das, R. V. Rajakumar, M. I. Rahman, A. Pal, F. H.P. Fitzek, O. Olsen, R. Prasad: Low complexity residual phase tracking algorithm for ofdm-based wlan systems. pp. 54–59 (Aalborg, Denmark, September, 2005)
  14. Sharif, M., Gharavi-Alkhansari, M., Khalaj, B.H.: On the peak-to-average power of OFDM signals based on oversampling. *IEEE Trans. Commun.* **51**(1), 72–78 (2003)
  15. Shi, K., Zhang, N.: Single stream phase tracking during channel estimation in a very high throughput wireless mimo communication system. US Patent 8494075B2 (July 23, 2013)
  16. Tseng, C.C., Liu, C.: Complementary sets of sequences. *IEEE Trans. Inf. Theory* **18**(5), 644–652 (1972)